Journal Pre-proof

Experimental study of chemical evolution and isotope fractionation of Cl and Br in pore water expelled during strong clay compaction

Jessica Strydom, Jérôme Sterpenich, Dragan Grgic, Antonin Richard, Hans G.M. Eggenkamp, Pierre Agrinier, Pascale Louvat, Régine Mosser-Ruck, Patrick Gaire, Eric C. Gaucher

PII: S0883-2927(22)00078-6

DOI: https://doi.org/10.1016/j.apgeochem.2022.105274

Reference: AG 105274

To appear in: *Applied Geochemistry*

Received Date: 26 November 2021

Revised Date: 17 March 2022

Accepted Date: 18 March 2022

Please cite this article as: Strydom, J., Sterpenich, Jéô., Grgic, D., Richard, A., Eggenkamp, H.G.M., Agrinier, P., Louvat, P., Mosser-Ruck, Ré., Gaire, P., Gaucher, E.C., Experimental study of chemical evolution and isotope fractionation of Cl and Br in pore water expelled during strong clay compaction, *Applied Geochemistry* (2022), doi: https://doi.org/10.1016/j.apgeochem.2022.105274.

Experimental study of chemical evolution and isotope fractionation of Cl and Br in pore water expelled during strong clay compaction

Jessica Strydom[a], Jérôme Sterpenich[a], Dragan Grgic[a], Antonin Richard[a], Hans G. M. Eggenkamp[b,d], Pierre Agrinier[b], Pascale Louvat[b], Régine Mosser-Ruck[a], Patrick Gaire[a], Eric C. Gaucher[c,e]

[a]Université de Lorraine, CNRS, GeoRessources, CREGU, F-54000 Nancy, France.

[b]Université Paris Cité, Institut de Physique du Globe de Paris, 1, rue Jussieu - 75238 Paris cedex 05, France

[c]Total CSTJF, Avenue Larribau, Pau, F-64000, France

[d]Mathematisch-Naturwissenschaftliche Fakultät, FB Geowissenschaften, Eberhard Karls Universität Tübingen, Schnarrenbergstraße 94-96, D-72076 Tübingen, Germany

[e]Institute of Geological Sciences, University of Bern, Baltzerstrasse 1+3, CH-3012 Bern, Switzerland

Corresponding author's email: jerome.sterpenich@univ.lorraine.fr

Keywords:
Clay compaction
Isotope fractionation
Chlorine
Bromine
Ultrafiltration

ABSTRACT

In sedimentary basins, clay compaction by burial can lead to fluid overpressure and is suspected to also generate fresh waters, but few geochemical tracers are available to assess this process both qualitatively and quantitatively. Our objective was to carry out experiments on the chemical - and halogen (Cl, Br) isotope evolutions of pore water expelled during clay compaction. For this, the smectite-rich bentonite MX80 and an illite-rich marl (Sainte-Suzanne) were equilibrated with ocean water. During two compaction experiments under high fluid pressure (45 MPa), mechanical stress (up to 150 MPa) and temperature (up to 150 °C), it was found that the chemistry and isotope behavior is considerably different between the swelling clay and the non-swelling clay.

We saw a general decrease of the cat- and anion concentrations in the expelled water, for swelling clay while its concentration slightly increases in the remaining pore fluid. This was not the case for non-swelling clay. More freshening of the expelled water occurred during the compaction at higher temperature.

We also observed a larger range of isotopic variation for Br (δ^{81}Br from 0.9‰ up to 1.5‰) than for Cl (δ^{37}Cl from -0.5‰ to -0.1‰) in the compaction experiments. During the compaction of illite-rich marl, no significant variation of Cl isotope (δ^{37}Cl close to 0‰) was observed while the δ^{81}Br value of the expelled water showed the same general increase (from 0.9 ‰ up to 1.5‰) as during the compaction of smectite-rich bentonite.

We observed limited mineralogical transformations in terms of dissolution/precipitation processes. Therefore the surface chemistry of the clay in combination with decreasing porosity, in part, drive the anion and isotope evolution. We propose that significant retention of Cl and Br in the pore water of the compacted smectite-rich bentonite is indicative of ultrafiltration and

that that Cl and Br isotopes are promising tracers to consider when tracking the origin of low-salinity formation waters in sedimentary basins.

1. INTRODUCTION

Among the processes explaining fluid overpressure in sedimentary basins, the clay compaction is one of the most significant. Clay compaction produces fresh water by the physical process of ultrafiltration (Coplen and Hanshaw, 1973; Kharaka and Berry, 1973; Haydon and Graf, 1986; Phillips and Bentley, 1987; Demir, 1988). The microstructure of the clay rocks creates a very tortuous and electrically charged pore network inducing long pathways and ionic repulsions trapping the ions in the clay rocks (Melkior et al., 2009). Recently, two types of water produced during burial of clay formations were clearly described by Tremosa et al. (2020). The first is produced by mechanical compaction when adsorbed water layers are expelled. The second is produced by the mineralogical transformation of the clays due to the increasing temperature. These two types of water dilute the former formation waters. The term formation water describes water that saturates sedimentary rocks (among them deep oil or gas reservoir rocks).

Migration of free-flowing formation water is an important factor in mass movement/transport and diagenesis due to the inevitable chemical reactions with rocks along its migration path Bethke and Marshak (1990). Studying formation waters is beneficial to understand the original source of the waters, which could potentially link to the origin of the hydrocarbon resources, the dynamics of low temperature geothermal systems and the formation of basin-hosted mineral deposits Garven (1995). Formation waters can range from very saline to remarkably fresh (low salinity or dilute) Solley and Chase (1983); Carpenter (1978); Hanor (1987). Dilution or freshening of formation waters are attributed to;

1. Ultrafiltration (the relative retardation of solutes with respect to flowing solution when passing through fine grained material
2. Condensate water (water produced from the condensation of water vapor present in hydrocarbon gas reservoirs when the pressure is reduced during production)
3. Mixing with external fluids (meteoric water or diluted continental waters (rivers, lakes))
4. Water-rock interactions
5. Clay mineral transformation/dehydration.

The hydrophilic and unreactive nature of chloride and bromide ions causes them to remain in solution with very little incorporation into minerals (Davis et al., 1998; Worden, 1996). Therefore, by studying Cl and Br anions as tracer conservative elements, one can follow the fluid transport without much interference from water-rock interactions with the exception of evaporates and organic matter (Richard et al., 2011; Kendrick et al., 2011; Pusch et al., 1990). Because dissolved Cl and Br are so unreactive, it is also interesting to consider their stable isotopes to understand what physical processes are influencing the fluid evolution. The stable isotopes of both chlorine (^{35}Cl and ^{37}Cl) and bromine (^{79}Br and ^{81}Br) are fractionated by natural and anthropogenic processes during their cycling between reservoirs. Stable isotope ratios of Cl have been used to describe various physical processes that could have contributed to formation water composition, including salt precipitation (Eggenkamp et al., 1995), ion filtration (Phillips and Bentley, 1987), ion exchange (Musashi et al., 2004) and diffusion (Eggenkamp and Coleman, 2009; Beekman et al., 2011). With fewer focused studies, the behavior and application of Br stable isotope ratios is still not well understood (Shouakar-Stash et al., 2007; Stotler et al., 2010). From previous literature, we know that the δ^{37}Cl values of formation waters are usually negative and can vary significantly, down to -8‰ (Agrinier et al., 2019). From the few studies that have measured the isotopic ratios of Br in formation waters, the δ^{81}Br values are mostly positive and vary up to +4‰ (Eggenkamp, 2014a). Both being halogens, Cl and Br have originally been assumed to show similar type of isotopic variations. As the capabilities to measure Cl and Br isotopes have developed, it has become clear that the stable isotopes of these anions fractionate differently despite their similar chemical behavior. The fractionation of Cl isotopes by the process of diffusion has been clearly illustrated in fine-grained low-porosity clay-rich materials (Kaufmann et al., 1984; Phillips and Bentley, 1987; Lavastre et al., 2005). There seems to be a decreasing trend for δ^{37}Cl with increasing depth (Agrinier et al., 2019, 2021). The fractionation of Br isotopes due to diffusion has only been studied experimentally where it has been shown to correlate with the diffusion of Cl (Eggenkamp and Coleman, 2009). It has been assumed previously that due to the larger ionic radius and higher atomic mass, Br isotope fractionation should be roughly half as large as Cl isotope fractionation (Eggenkamp (2014b)). δ^{81}Br trends with increasing depth have not been studied. Interestingly, comparing published δ^{37}Cl and δ^{81}Br values of natural formation waters, those samples with very negative Cl isotope ratios often show surprisingly positive Br isotope values. It was suggested that these values might be the result of ion filtration through semi-permeable clay membranes as a consequence of clay surface charges (Tournassat and Appelo, 2011; Coplen and Hanshaw, 1973; Kharaka and Berry, 1973; Campbell, 1985).

For this study, we are experimentally investigating ion filtration effects on ocean water by means of a high pressure and temperature compaction experiment. It has been specifically designed to extract pore water volumes large enough to measure chlorine and bromine stable isotope composition, together with the evolution of pore water chemistry during stepwise pressure and temperature increases, in order to follow the effect of clay compaction. We compare two distinctly different clay-rich materials. The first, MX80, is a well-studied and well-characterized clay with high content of swelling clay minerals (smectite). The second material used is the Sainte Suzanne marl (SSM) from the Aquitaine basin (France) and is of interest as it acts as a flow and thermal barrier between the upper (less saline) and lower (more saline) Lacq reservoirs (Bahnan et al., 2020). The SSM contains a smaller quantity of clay minerals, which are mostly non-swelling in nature (predominantly illite-rich). Expulsion of water from the compaction of the clay-rich SSM could have contributed to dilution of the aquifer water in the upper Lacq reservoir according to Bahnan et al. (2020).

2. MATERIALS AND METHODS

2.1 Starting materials

The two materials selected for this experiment were MX80 smectite clay (450 g, MX80 experiment) and powdered Sainte-Suzanne marl (550 g, SSM experiment) from the Aquitaine basin (borehole LA 101; latitude 43.420648° and longitude -0.619980°). MX80 is well characterized and widely studied in numerous compaction studies (Sauzéat et al., 2001; Neaman et al., 2003; Mondol et al., 2007; Karnland et al., 2007). It consists of 75 wt% Na-Ca montmorillonite, 15 wt% quartz, 5-8 wt% feldspars (plagioclase and microcline) with lesser amounts of kaolinite, phlogopite, calcite, siderite, pyrite and organic carbon (Bradbury and Baeyens, 2003). In contrast, the clay component of the SSM, as characterized with SEM and XRD, consists of 61 wt% illite, 16 wt% quartz, 10 wt% feldspars (anorthite and albite), 7 wt% kaolinite, 3.5 wt% calcite, while the remainder of the rock comprising cristobalite and pyrite. In terms of the particle size of the materials, approximately 80% < 63 µm for MX80 and around 90% < 63 µm for SSM. Due to the high smectite content, the MX80 has a brut cation exchange capacity (CEC) of 70 meq/100g while the brut CEC for SSM is 9.8 meq/100g.

2.2 Experimental setup

In this study, two long-term experiments using two distinctly different clay-rich materials were carried out at GeoRessources laboratory, Vandoeuvre-lès-Nancy, France. A high stress/fluid pressure/temperature oedometric type cell was designed to experimentally simulate the diagenetic processes (fluid and heat flow, mechanical and chemical compaction) involved in the production of formation water from a saturated clay sample under deep burial conditions (around 6 - 7 km deep). Oedometric tests simulate the one-dimensional (vertical) deformation and drainage conditions: no lateral displacement of the cylindrical sample is possible, but the sample can swell/compress vertically in response to changes in axial (vertical) stress σ_1. For this experiment an oedometric cell, with internal dimensions of 10 cm diameter and 10 cm height, is connected to a set of pressure pumps for generating both pore fluid pressure (Pi) at both sample sides to allow drainage conditions, and a vertical stress up to 45 MPa and 150 MPa respectively, which can be individually controlled to induce the desired effective vertical stress to the sample (σ_1'= σ_1- P_i). Fig. 1 shows the experimental setup for the study: the oedometric cell [A], the oil-pressure generator (for the axial stress) [B], the fluid circulation system [C], the control and data acquisition systems [D], the system for heating control [E]. The oedometric cell is encased by two thermal heating rings to regulate the temperature up to 150°C. An inlet/outlet for fluid from the pore pressure generator pumps are positioned at both the top and bottom of the cell. Two 3 mm thick porous plates (retaining 98% of particles > 16µm) sit on opposite sides of the sample. The fluid can therefore uniformly percolate into/out of the sample. Because of valves placed between the pressure generator pumps and the inlet/outlet of the cell, flow can occur in both directions. The pore pressure generator pumps [C1 & C2], each with a capacity of 100 mL, can apply a constant fluid flow (0.00001–30 ml/min) or a constant fluid pressure. The data acquisition system allows for recording both the axial stress (σ_1) and the pore fluid pressure (P_i). Axial deformation is recorded from an externally fitted linear variable differential transformer (LVDT) sensor. The volumes of fluids in both of the pore pressure pumps are also continuously recorded thus allowing the calculation of the water and chemical mass balance of the system.

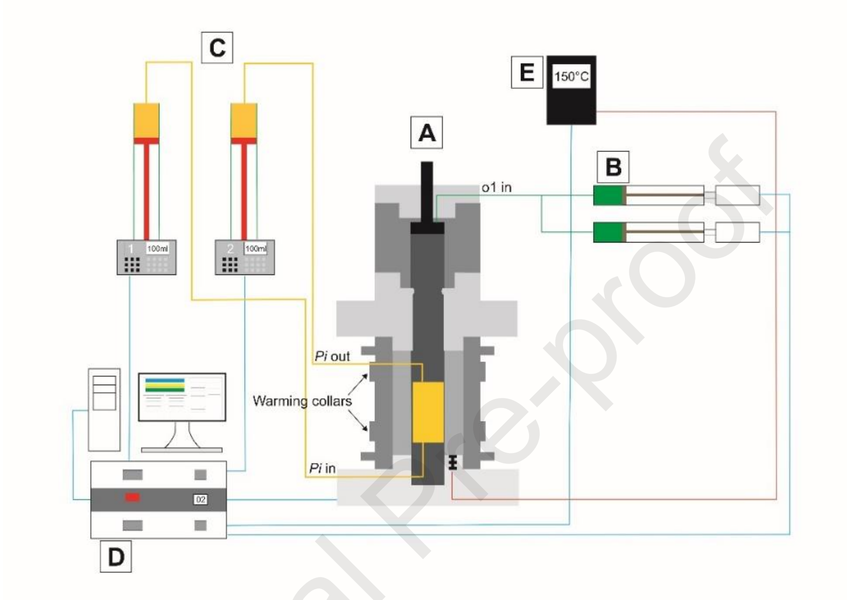

Figure 1: Illustration of the experimental system showing the compaction (oedometric) cell [A] and various operation systems: the oil-pressure generator (for the axial stress) [B], the fluid circulation system [C], the control and data acquisition systems [D], the system for heating control [E].

2.3 Experimental protocol

The compaction protocol followed a series of axial stress and temperature steps for up to 200 days. This study was not attempting to reproduce a specific basin or reservoir, therefore common values for axial load and thermal gradients and a constant pore pressure were selected. For the duration of the experiment the pore pressure was maintained at 45 MPa while the axial stress was increased from 45.5 MPa to 150 MPa (maximal effective stress: 105 MPa) by increments of ~ 25 MPa. Temperature was increased from room temperature to 150 °C by increments of 30°C.

Filtered natural Atlantic Ocean water (0.1 µm) sampled of the coast of Bidart (France), was used for both experiments. The chemical composition of the ocean water is given in Table 1. The experimental conditions were progressively applied in the following order:

1. Application of a low axial stress ($\sigma 1$ = 1.5 MPa) for the sample saturation;
2. Hydration of the dry powdered material in the cell from both the top and bottom inlet at low injection pressure of ~1 MPa;
3. When the clay was fully hydrated (i.e. no more fluid was taken up by the clay material), a pressure gradient was applied (from the bottom to the top) until the bottom injection pump C1 was emptied, thus allowing water flow and complete chemical equilibration. At the end of this step, the injection pump at the bottom C1 was isolated from the oedometric cell with a valve, so that no new water will be injected during compaction. The injection pump at the top C2 was almost entirely emptied; only a small amount ocean water was kept to maintain pore pressure in the sample and to collect the expelled water during the experiment.
4. Application of the vertical stress ($\sigma 1$ = 45.5 MPa) using a loading rate of 0.001 MPa/s;
5. Application of the interstitial pressure (Pi = 45 MPa) using a loading rate of 0.002 MPa/s;
6. Beginning of the stepwise incremental increase of the vertical stress ($\sigma 1$ max = 150MPa) using a loading rate of 0.001 MPa/s and simultaneous application of incremental temperature increase.

The duration of the steps varied between two and four weeks to allow for the stabilization of the axial compaction (deformation) curves.

Expelled fluid was sampled as soon as the minimum required volume of 2 ml has accumulated in the collection pump C2. Fluid was not expelled at each step. The last sampling was done at step 3 (105 MPa, 90°C) for SSM and at step 4 (125 MPa, 120°C) for MX80.

2.4 Analytical methods

Chemical and isotopic analyses of fluids

To measure variations in the fluid composition over time, expelled fluid was sampled for each stress step. Upon collection;

1. the pH was measured;
2. the sample was filtered (0.025 µm) to remove any suspended clay particles, and
3. split into two aliquots.

A proportion was diluted and acidified (2% HNO_3) for ICP-MS analysis and the remainder was refrigerated in an airtight flask for later isotope analyses. Elemental concentrations were assessed using an Agilent 7900 quadrupole ICP-MS at the Institut du Globe de Physique de Paris (IPGP), France and Cl isotope analyses were carried according to Kaufmann et al. (1984); Eggenkamp (1994, 2014b) and Godon et al. (2004). Repeated analysis of Atlantique 2 seawater reference (Godon et al., 2004) gave δ^{37}Cl reproducibility of ± 0.03‰ (1σ, n = 48). For the extraction and measurement of Br isotopic content, the protocol thoroughly described by Eggenkamp and Louvat (2018) was closely followed. Br is extracted by distillation in the presence of nitric acid and trapping it in an ammonia solution. The distillation method has been shown to be an effective alternative to the customary extraction by ion exchange chromatography on anion exchange resin (Louvat et al. (2016)) in cases where high Cl content can be problematic to Br extraction due to supersaturation of the resin by Cl. A dilute nitric acid solution will oxidize Br^- to Br_2 but will not oxidize Cl^- therefore a solution containing little to no Cl^- can be produced from solutions with large Cl/Br ratios, by the acid distillation method. Trapping the solution in a strongly reducing alkaline environment such as an ammonia solution disproportionates the Br_2 to Br^- and BrO_3^- in a ratio of 5:1. Due to the reducing nature of the ammonia solution the BrO_3^- is then reduced to Br^-. Enough sample should be used to provide a minimum of 20 µg Br. For ocean water, the distillation requires that 1 ml HNO_3 (69%) is added to ~ 0.5 ml sample plus 3.5 ml de-ionized water, immediately closed up and vigorously boiled over a low heat source for 8-10 minutes until the 1 ml of 0.5 M NH_3 on the trapping end of the distillation has doubled in volume - i.e. 1 ml has been distilled. This solution is then analyzed with a Thermo Neptune multi collector inductively coupled plasma mass spectrometer. An average of 5 repeated measurements was used to calculate the δ^{81}Br, giving a reproducibility of ±0.11‰ (2σ, n = 60).

After completion of the experiments, the compositions of the two compacted cores were characterized by semi–quantitative X-ray diffractometry (XRD) at GeoRessources laboratory. XRD patterns were collected on a D8 Advance Bruker AXS diffractometer at 35 kV and 45 mA with non-monochromatic CoKα radiation (λ = 0.17903 nm), with an iron filter to suppress the Kβ emission, and equipped with a LynxEye fast linear detector. Intensities were recorded from 3 to 75°2θ with a 0.035°2θ step using a 3s counting time per step. For the fine clay fraction (< 2 microns), intensities were recorded from 2 to 40°2θ with a 0.02°2θ step using a 4s counting time per step. Data reduction and analysis were performed with the EVA software (DIFFRACplus from Bruker) and diffraction peaks were identified by comparison with powder diffraction files (PDF2 database from the International Center for Diffraction Data, ICDD).

3. RESULTS

3.1 Physical parameters

Figure 2 represents compaction curves for the two experiments (the convention of positive compressions for stress and displacement is used) and Table 1S (Supplementary Material) shows the volumes of water that were collected during the two experiments. During the hydration and equilibration step, the vertical stress was equal to 1.5 MPa to compensate the swelling pressure of the MX80 due to the strongly adsorbed interlayer water, which means that no swelling (dilatant deformation) could be observed. On the contrary, compaction was observed. In the absence of swelling clay minerals, the SSM compacted more (25%) than the MX80 (15%). This is due to the swelling pressure maintained by the MX80. Both materials absorbed similar volumes of water (about 100 mL) and for both the materials the largest volumes of water were expelled during the earlier compaction steps. Water was not expelled at each step. At the end of experiment 30% of the initial volume of absorbed water was expelled for the MX80 experiment and 52% for the SSM experiment.

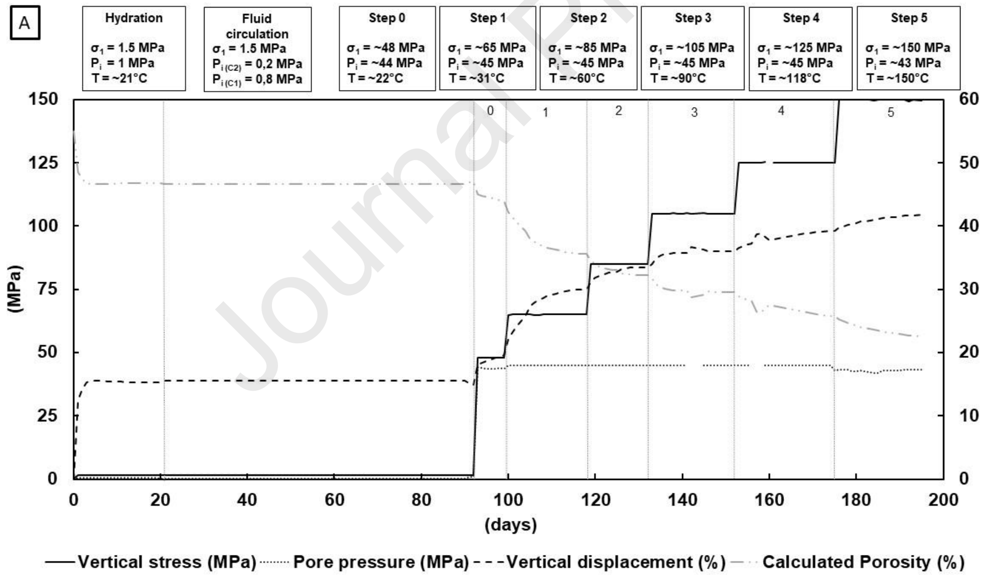

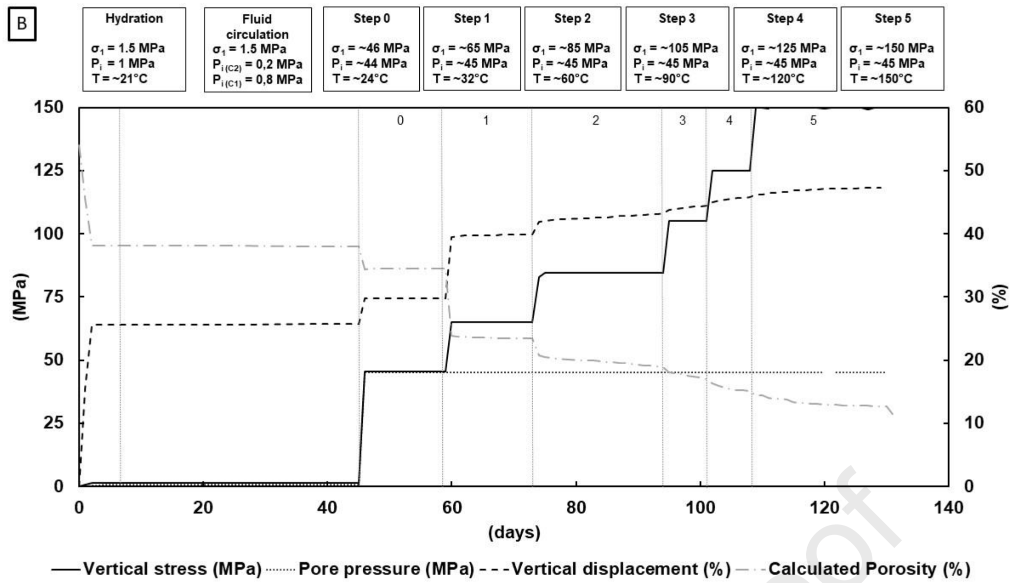

Figure 2: Compaction curve as a function of time for MX80 (A) and SSM (B). The same vertical stress, pressure and temperature increments were followed in both experiments. The pore pressure was maintained at 45 MPa while the vertical stress was increased from 45.5 MPa to 150 MPa by increments of ~ 25 MPa. Temperature was increased by increments of 30°C from step 1.

The compaction leads to a variation of the sample porosity which cannot be measured during the experiment but only estimated from the bulk volume variations of the system. The decrease in total porosity, calculated from the volumetric mass densities, occurs mainly during the step at 65 MPa and 30°C. At the end of experiment the porosity drops from 55% to 22% for MX80 and from 54% to 16% for SSM. Mercury porosity measurements performed after experiments give 8% of free porosity and 9% of trapped porosity for a total of 17% of connected porosity for MX80. The values are 4.4%, 3.6% and 8% respectively for SSM. This means, a large proportion (53% for MX80 and 45% for SSM) of the porosity is trapped (i.e. pores no longer have a continuous path towards the sample surface). Intrusion of mercury into a cavity is controlled by the size of the pore throat radius while the radius of the cavity and its connectivity controls extrusion of mercury from the cavity. The median pore diameter is 7 nm for MX80 and 9 nm for SSM. The discrepancy between the mercury porosity and calculated porosity can be attributed to the absorbed water content present in the clay.

The CEC slightly increases for MX80 to reach 77 mEq.100g^{-1} (70 mEq.100g^{-1}initially) and doesn't change for SSM and stays at 9.8 mEq.100g^{-1} after experiment. This could be due to the slight mineralogical changes observed during MX80 compaction.

3.2 Mineralogy

X-ray diffractograms are shown in Figure 3 and 4. Some modifications of the global mineralogical composition of solids has been observed after both experiments. For MX80, the main transformation concerns the montmorillonite. Its interlayer composition changes after experiment characterized by an enrichment in Na and K (shift of the (001) peak toward higher 2θ angles). Ca is expelled from the crystallographic structure. A possible but limited illitization could be envisaged. Phlogopite is likely altered if considering that the amount of quartz and calcite has not changed during experiment (based on the comparison of the intensities of their peaks). Plagioclases crystallize (albite and anorthite). Peaks of gypsum are not observed on the diffractogram after experiment, it probably dissolves. Two peaks around 51.5 °2θ and 62.6°2θ were difficult to attribute to the phases already identified. They could match with pyrrhotite.

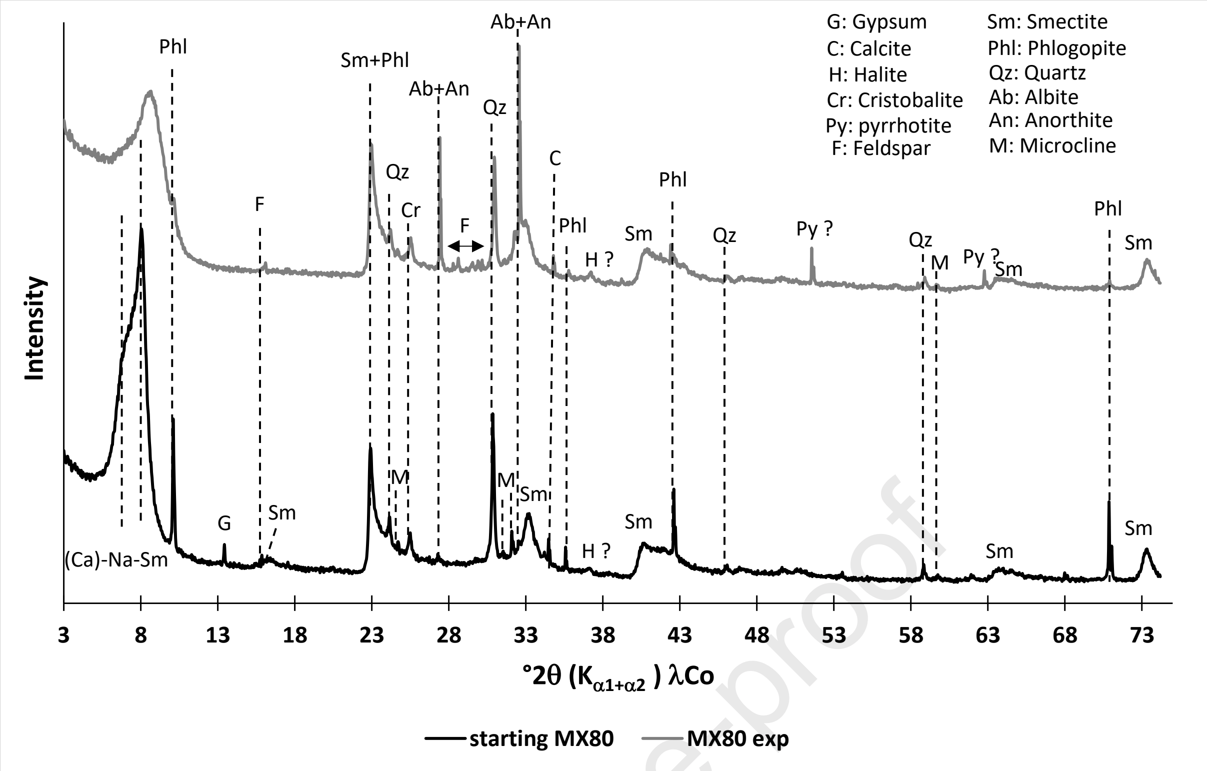

Figure 3: X-Ray diffractograms of the MX80 sample before and after experiment (starting MX80 and MX80 exp respectively).

For SSM, assuming that the quartz is not affected during the experiment (intensity of the main quartz peak identical on the two diffractograms of figure 4), a significant decrease in the intensity of kaolinite, illite and anorthite peaks can be attributed to a drop in the amounts of these three minerals during experiment. The most altered mineral would be kaolinite. Low intensity peaks of chlorite appear on the diffractogram of the sample after experiment. Calcite and pyrite seem unaffected. It has to be noticed that it is not possible to determine the moment when the mineralogical transformation occur during experiment. It can be envisaged that the main transformations happen at higher temperatures thus rather at the end of experiment, because kinetics are more favorable.

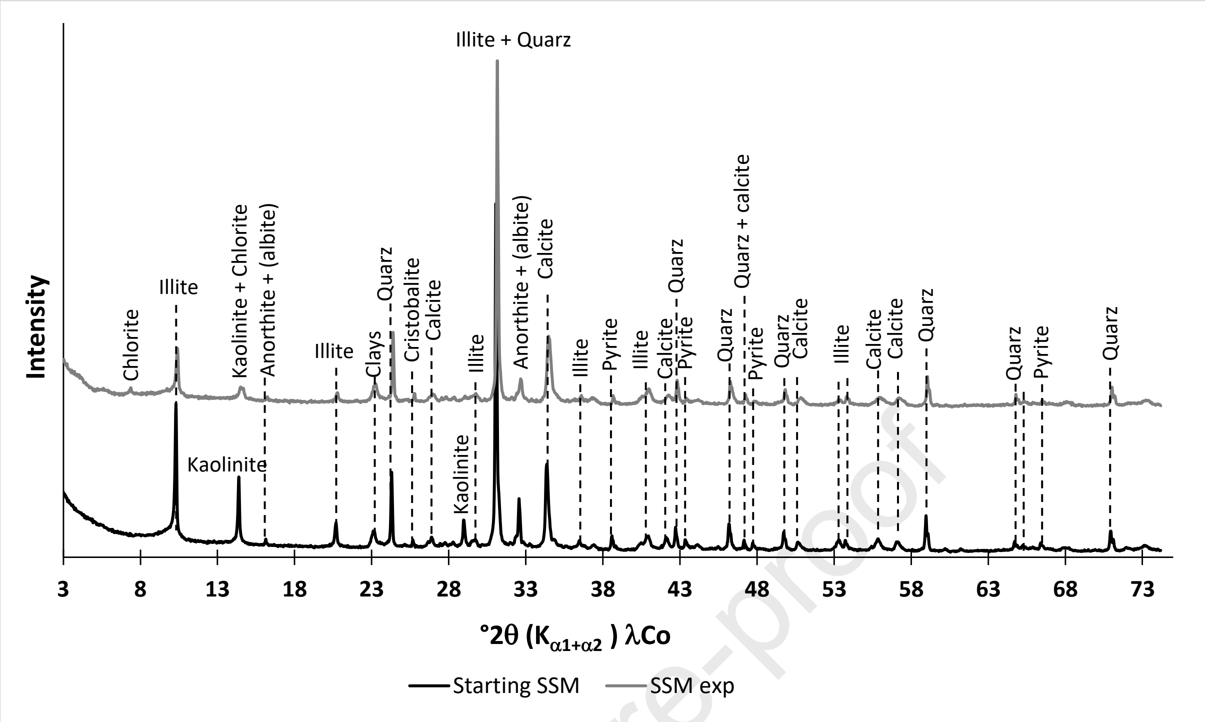

Figure 4: X-Ray diffractograms of the SSM sample before and after experiment (starting SSM and SSM exp respectively).

3.3 Fluid chemistry

Table 1S (Supplementary Material) shows the volumes of water that were collected during the various compaction steps. 96.3 ml of ocean water were absorbed and only 28.9 ml of water (30%) were expelled during the compaction experiment for MX80 experiment. For SSM experiment, the absorbed volume was 107.5 ml but more than 52% (56.3 ml) was expelled. During compaction step 1, two separate samples were collected in the 14-15 days at the same pressure and temperature. For the next steps, the volume collected were significantly lower and some steps didn’t expel any water.

For the MX80 experiment, the ocean water is first cycled through the clay under a minimum load of 1.5 MPa to reach the best close to equilibrium state between the clay and ocean water. The resulting water is called “initial water” in (Table 1). The initial water is significantly different from the Bidart water: the Cl, Br and Na concentrations increase by around 10%.

Interestingly, this is not the case for K. A more pronounced enrichment is observed for Ca and S maybe due to fast equilibrium with sulfate and carbonate minerals. Si, and Mg are less concentrated in this initial water. The first step of compression to 45 MPa leads to the more pronounced variations of the water chemistry. The concentrations of Na, K, Mg, Ca, Cl, Br and S increase by 35 to 40% by comparison with the Bidard composition. Then, the following steps of T and P increase roughly lead to a progressive decrease of the concentrations of Na, K, Mg, Cl and Br in the expelled solution. At the end of experiment, the salinity expressed by the ionic strength I of the expelled solution has dropped from 0.7 to 0.37. The pH of the initial solution is 8.1 and we can observe a slight drop of the pH during experiments with values ranging between 7.7 and 8.0.

Concerning the SSM experiment, the results are quite different. The initial water assumed to be in equilibrium with the marl, shows increasing concentrations for Ca, S and in to a lesser extent K, likely to be attributed to chemical equilibrium with carbonate and sulfate minerals for calcium and sulfur. The steps of increasing P and T lead to slight variations of the solution chemistry. Notice that the last solution was collected at 105 MPa and 90°C. No more water was expelled during the last two steps. The pH of the solution slightly decreases from 8.2 to 7.6 during the different steps of the experiment.

Table 1 : Chemical composition of the aqueous solution sampled in the MX80 and SSM experiments. I is for ionic strength calculated from major elements. Concentrations in mmol.L^{-1}.

	Sample description	I	pH	Na	K	Ca	Mg	Si	S	Cl	Br
	Bidart	0.697	8.1	481.9	10.1	10.7	54.6	1.16	24.7	524.1	0.88
MX80	Initial pore water*	0.746	7.7	538.2	8.43	17.73	42.74	0.41	31.9	570.7	0.97
	45.5 MPa	0.948	7.8	649.5	13.90	14.28	75.27	0.28	33.1	738.6	1.24
	65 MPa & 30°C	0.728	7.7	548.6	6.48	20.36	27.92	0.96	48.9	497.7	0.81
	65 MPa & 30°C	0.754	7.7	576.1	5.49	21.67	24.73	1.04	52.5	514.6	0.83
	85 MPa & 60°C	0.653	7.9	501.4	4.48	17.88	20.34	1.26	47.7	436.2	0.71
	125 MPa & 120°C	0.370	8.0	296.5	2.38	8.31	9.36	2.45	23.6	238.1	0.38
SSM	Initial pore water*	0.710	8.2	497.2	12.3	25.9	37.3	0.33	36.3	506.4	0.78
	65 MPa & 30°C	0.705	8.1	488.7	11.4	25.5	39.2	0.46	35.2	503.1	0.77
	65 MPa & 30°C	0.726	7.9	507.2	11.7	25.3	40.8	0.40	35.4	520.6	0.80
	85 MPa & 60°c	0.705	7.9	490.4	12.0	25.3	38.7	0.80	33.6	504.3	0.78
	105 MPa &90°C	0.746	7.6	521.1	13.1	25.0	40.5	0.58	36.5	541.2	0.84

**The initial pore fluid concentration refers to the re-equilibrated ocean water composition, i.e. the composition of the ocean water after it has circulated through the clay before the compaction.*

3.4 Cl and Br concentrations and isotopes

The evolution of both concentrations and isotopes ratios for Cl and Br are given in Fig. 5 for the MX80 and SSM experiments. Fig 6 shows that Cl and Br concentrations are correlated. The range of variations is however more marked in the MX80 experiment than in the SSM experiment. The δ^{37}Cl value of the initial Bidart ocean water is -0.12‰ (±0.03) and the Cl content is 524 mmol.L^{-1}. After equilibration with MX-80 the first notable Cl isotope variation occurred.

The δ^{37}Cl of the re-equilibrated ocean water has decreased to -0.2‰ (±0.03). With pressurization to 45 MPa, δ^{37}Cl values reach 0.02‰ (±0.02) in the first water expelled with a significant enrichment in Cl (738 mmol.L^{-1}). The δ^{37}Cl values then decreased with increasing pressure and temperature, together with the Cl concentration. The variation that occurs at 65 MPa (step 1) is noteworthy. As mentioned before, two samples were collected during this step. In the first water expelled at 65 MPa, the $\delta^{37}Cl$ was -0.24‰ (±0.03). After 14 days at the same pressure and temperature conditions, the $\delta^{37}Cl$ value has decreased to -0.45‰ (±0.03), but keeping a comparable Cl concentration. Following the variation at 65 MPa and 30°C, no more significant fractionation occurred in the water expelled from the MX-80 compaction, but the last step is characterized by the lower Cl content (238 mmol.L^{-1}).

The SSM experiment show very weak variations of both Cl content and $\delta^{37}Cl$.

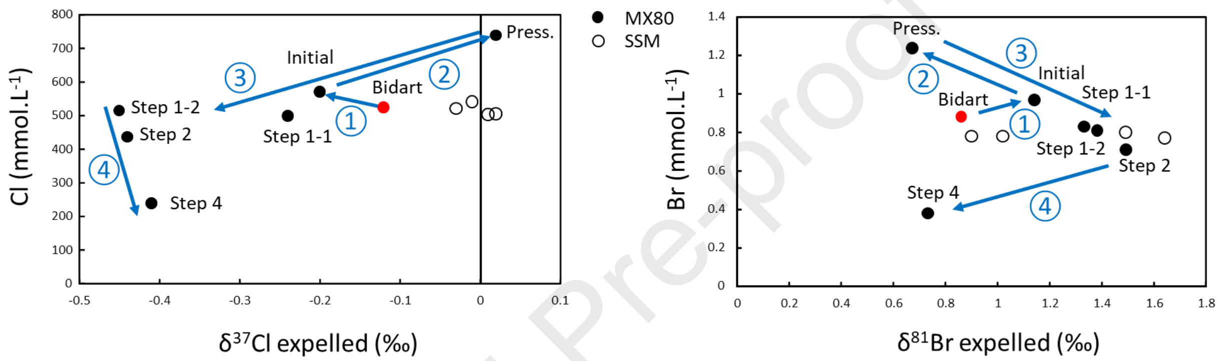

Fig. 5: Concentrations and isotope compositions of Cl and Br in the MX80 and SSM experiments. The different steps of compaction are given for MX80. "Press." means pore pressurization at 45 MPa. "Bidart" corresponds to ocean water sampled at Bidart (France). "Initial" corresponds to the values of equilibrated water before the beginning of compactions steps. The blue arrows correspond to the different successive mechanisms described in the discussion.

Regarding Br isotopes, two important observations can be seen from Fig. 5. Firstly, the range of Br variation observed, is larger than the range of variation of Cl and secondly, $\delta^{37}Cl$ values are negatively correlated with the $\delta^{81}Br$. The initial Bidart ocean water has a $\delta^{81}Br$ value of 0.86‰ (±0.07).

A delta value of 0.86‰ is highly unlikely for ocean water (Eggenkamp et al. (2019)). Preliminary data obtained from halite samples suggested that the values for the Br isotopes should not be higher than 0.5‰, the value of the reference standard from the IPGP. A possible bad distillation may have happened, but seems unlikely as to increase the value by 0.86‰ is so large that something very strange must have occurred during distillation that it could not have gone unnoticed. What however may be possible is that the high value is related to the sample location, which was along the coast: Br isotopes can change because of interaction with organic material, but the magnitude of fractionation, is not known and has also never been studied in detail. Little attention is given to this problem. The purpose of the study is after all to course the changes in isotope ratios due to compaction, and in principle for that study, the primary isotope ratio of the sample is not important, only the changes that occur during the experiments.

After the equilibration with MX80, the first significant variation was observed as the δ^{81}Br of the initial water reached 1.14‰ (±0.01). With pressurization to 45 MPa the δ^{81}Br decreases to 0.67‰ (±0.12). The significant variation of Cl isotopes that is observed for the two samples collected during the step at 65 MPa & 30°C, is not seen for Br. The δ^{81}Br value for the first sample at these conditions was 1.38‰ (±0.05) and for the next, 14 days later, was 1.33‰. (±0.14). When compaction of the MX-80 progresses, the δ^{81}Br values continue to increase up to 1.5‰ (±0.01) at 85 MPa & 60°C before it decreases to 0.7‰ (±0.22) in the water expelled at 125 MPa & 120°C.

During SSM compaction the range of Br isotope variation that occurs shows a similar range as observed during MX-80 compaction (Fig. 5**)**. In comparison, during the SSM compaction, the δ^{81}Br value changes from 0.86‰ (±0.07) in the Bidart ocean water to 1.02‰ (±0.12) after it has been re-equilibrated with the clay (initial pore water). A significant shift to 1.6 ‰ (±0.12) is observed in the water expelled at 65 MPa and 30°C. In the second sample collected at the same pressure and temperature conditions, 14 days later, the δ^{81}Br is 1.5‰ (±0.12). At

85 MP and 90°C, the $\delta^{81}Br$ value decreases suddenly to 0.9‰ (±0.07) before the value increases to 1.5‰ (±0.10) in the last expelled water collected.

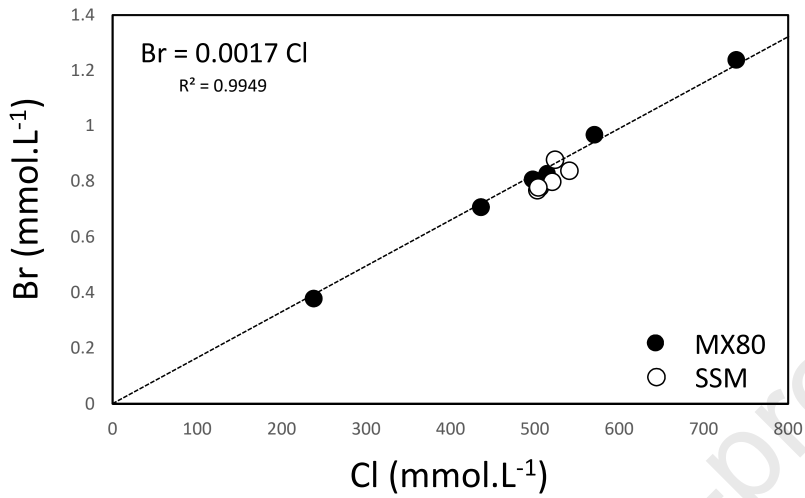

Fig. 6. Br and Cl concentrations in the expelled fluid of MX80 and SSM experiments.

4. DISCUSSION

To interpret the results of the compaction experiments, we have to decipher the different mechanisms that are responsible for the chemical and mineralogical evolution of the system. XRD analyses show that the mineralogical transformations remain limited. The main transformation concerns the MX80 experiment with a part (10 to 15%) of the smectite being transformed in sodic montmorillonite, kaolinite and albite. In the SSM experiment, experimental data predict a weaker reactivity of the system. This is well confirmed by the chemistry of the expelled water that remains roughly constant whatever the experimental conditions applied.

Thus, assuming limited mineralogical transformations in terms of dissolution/precipitation processes, the evolution of the chemistry of the solution is a result of either adsorption/repulsion on the negatively charged surface of clay minerals and/or elements trapping due to the decrease of clay porosity under compaction. This is especially applicable for elements such as halogens that are poorly incorporated in secondary minerals that could precipitate during the compaction.

Another important point is that the expelled volume is small by comparison with the remaining water (several percent at each step). Consequently, to better understand the behavior of elements, a mass balance has to be calculated to evaluate the bulk chemical composition of the pore water. Table 1S (Supplementary Material) presents the concentrations of halogens both in the expelled water and that calculated in the pore water. Notice that the mass balance is not performed for cations since they are more sensible to chemical reactions despite limited. When looking at the variations of Cl and Br concentration in the pore water, they remain very very low by comparison with that of the expelled water. That is to say that the chemical equilibrium between expelled water and pore water is never achieved in the experiment.

To understand the chemical and isotopic evolution of the system, a special attention has to be paid to the different types of pore water in clays, to the anion exclusion effect and to the evolution of the porosity with compaction leading to a change of the dominated transport of solute.

4.1 The diffuse double layer (DDL)

Clay minerals are characterized by their stacking of tetrahedral (T) and octahedral (O) sheets forming layers. The isomorphic substitution of cations in sheets (Si^{4+}-Al^{3+} substitutions in tetrahedron or Al^{3+}-Mg^{2+} substitutions in octahedron for instance) is responsible for permanent negative surface charge of clay minerals (Brigatti et al., 2013). The negative surface charge causes individual layers to accumulate in stacks and stacks to arrange in edge to edge or edge to face structures. This arrangement creates interlayer and interparticle spaces which can be filled by water. As a consequence of the surface charge, the whole water trapped in the clay porosity does not respect the electrical neutrality, especially in the vicinity of the clay surface (Revil and Leroy, 2004) where hydrated counterions (cations) are sorbed directly onto the negative particle surface mainly due to electrostatic interactions (Langmuir, 1918; Stern, 1924). In the diffuse layer, ions are more loosely attracted to the surface via Coulomb forces and can move in the fluid under the influence of electric attraction, thermal motion or concentration gradients.

So the interparticle layer is composed of the DDL and the free pore water. The concentration of counter-ions decreases with distance from the charged particle surface until there will be no distinction between the DDL and the free pore water. Smaller cations are prominent in interlayer and bound water while large anions dominate the free water fraction in the interparticle space. Anions with the greatest polarization potential (ability of an anion to be distorted by a cation) are preferentially adsorbed. This is usually the largest anions. The adsorbed ions are also governed by the composition and the ionic strength of the solution surrounding the particle (Brady and Weil, 2008). Cl and Br form sufficiently strong associations with cations to occur as neutral or positively charged ion pairs or clusters in the DDL (Neuzil and Person, 2017). According to Celejewski et al. (2018) chlorine can be included in the diffuse layer (bound water) while bromine will remain in the free water fraction as Cl preferentially associates with cations compared to Br (Eggenkamp and Coleman, 2009). Therefore, another consequence of the negative surface charge of clays concerns the transport of anions in the different porosities: because the anions are repulsed by negatively charged mineral surfaces, only a part of the total porosity is accessible for anions transport.

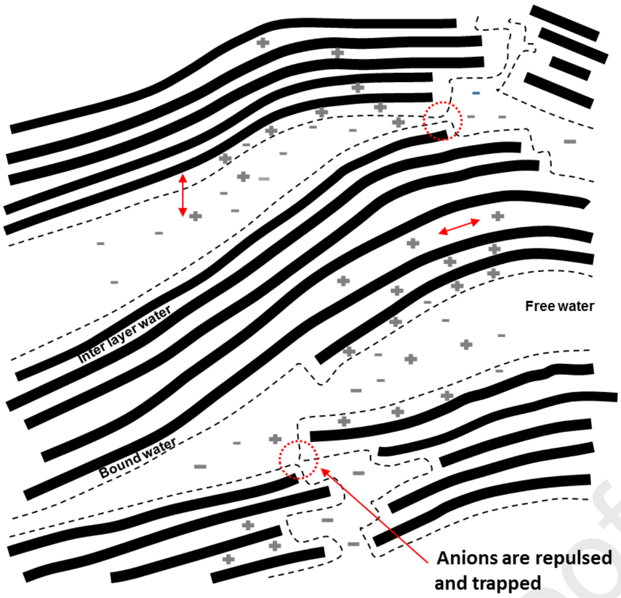

Figure 7: An illustration of the influence of the negative charge of clay particles on the physical and chemical morphology of clay rock pore spaces showing progressive expulsion and trapping and of the Cl and Br anions during compaction of negatively charged stacks. Red arrows represent the possible motions of ions in interlayer water and between free water and bound water.

4.2 Anion exclusion during clay compaction

During compaction of clays, the interparticle porosity will decrease first while the interlayer porosity will remain more or less constant (Muurinen et al., 2004). With increasing compaction, the interlayer porosity will also start to decrease (found to occur at bulk dry density >1300 kg/m^3, Van Loon et al., 2007). Due to the very narrow spaces created between clay particles within clay mineral stacks, the double layers in the interparticle porosity approach one another until they finally overlap. As a result, the negative electric potential in the interlayer space increases and all anions will be expelled from the interparticle porosity (Bolt and de Haan, 1982; Pusch et al., 1990; Wersin et al., 2004, Wigger and Van Loon, 2017). The resulting interparticle water now contains only cations while anions dominate the largest remaining interparticle porosity. At high compaction rates, the porosity mainly consists in interlayer porosity (Bourg et al., 2006), the interparticle porosity having almost entirely disappeared.

This phenomenon leading to the expulsion of anions of the decreasing porosity referred to as 'the anion exclusion effect'. In the case of high ionic strength of the pore solution, the majority of experimental or modeling studies show that the accessible porosity for anions increases. This is mainly explained by the fact that the volume of the DDL decreases due the high concentration of counterions in the solution able to counterbalance the mineral surface charge (Plecis et al., 2005). In addition to anion exclusion, overlapping DDL's also creates a charge barrier or blockage between converging clay particle stacks (Appelo et al., 2010). This prevents the passage of anions in free water. Therefore anions can either be trapped inside the diminishing pore spaces, and this is a function of the ion size, or forced to travel via longer transport routes through the clay layer, retarding transport, as illustrated in Fig.7. This is referred to as tortuosity (Melkior et al, 2009),

4.3 Transport in compacted clays

In fine-grained low-porosity clayey aquitards, where advective flow is low or absent, diffusion becomes the dominant transport mechanism. In clayey materials, the excess charge of clay minerals counterbalanced by ions of opposite charge induces electrostatic interactions that influence the mobility of ions in the solution. The mobility of ions is a function of the salinity and thus the ionic strength of the solution, its viscosity, the water content, the electrical charge of the clay surface, the temperature by the effect of Brownian movements, the pressure, the size and charge of the considered ions, the pore size of the medium and its tortuosity.

Electrostatic interactions increase with the salinity or the ionic strength of the solution resulting in slower diffusion of ions. The diffusion kinetics decreases when solution concentration increases (Schauble et al., 2003). Results from other diffusion experiments with clay-rich materials have shown that cation diffusion is normally enhanced compared to anion diffusion due to interlayer and DDL diffusion (Shackelford and Daniel, 1991; Sato et al., 1992; Kozaki et al., 1998; Molera and Eriksen, 2002; Van Loon et al., 2004; Van Loon et al., 2007, Descostes et al., 2008).

Temperature changes influence the rate of diffusion. Heat causes atoms to vibrate and vibration increases with increasing temperature. Therefore, increasing temperature will result in an enhanced diffusion coefficient (Desaulniers et al., 1986; Eggenkamp et al., 1994; Hendry et al., 2000; Hesse et al., 2006; Luo et al., 2014; Bernachot et al., 2017).

4.4 Isotope fractionation

Theoretically, due to the differences in masses, the different stable isotopes of an element would fractionate during the process of diffusion (Lindemann, 1921). Isotopic fractionation is defined as the relative partitioning of the heavier and lighter isotopes between two coexisting phases in a natural system, i.e. fractionation is a function of the relative difference of masses of the different isotopes. Fractionation is driven either by the equilibrium or kinetics of a system.

Therefore, the nature of the chemical bonds (Nygård et al., 2004) and the temperature (Urey, 1947) can influence isotopic fractionation. Fractionation normally decreases with increasing temperature (Richet et al., 1977; Schauble et al., 2003; Balan et al., 2019) and stronger chemical bonds generally preferentially involve the heavier isotope (Schauble, 2004*).* The fractionation in natural systems, such as in sediments, is dictated more by kinetics rather than equilibrium fractionations (solution and precipitation).

In order to assess element and isotopic fractionation during diffusion, there are three things that should be considered separately: (1) the relative atomic masses difference between Cl and Br, (2) the relative masses difference between ^{81}Br and ^{79}Br and (3) the relative mass difference between ^{37}Cl and ^{35}Cl. The Cl anion has a smaller radius than Br at 167 picometer and 182 picometer respectively. However the atomic mass of Br isotopes (78.9 and 80.9 $g.mol^{-1}$ for ^{79}Br and ^{81}Br respectively), are more than twice those of Cl isotopes (34.9 and 36.9 $g.mol^{-1}$ for ^{37}Cl and ^{35}Cl respectively). Therefore, Br is clearly expected to move slower, so fractionate less, than Cl during diffusion processes (Eggenkamp and Coleman, 2009).

4.5 Pore Water Evolution

The pore water is composed of the interlayer water, the trapped interparticle water, and the free interparticle water. It is this free pore water that is expelled during the experiments. While the DDL is dominated by cations, the Cl and Br anions will mostly be in the free water proportion of the pore water because they are largely excluded from the DDL. As a consequence only a part of the total porosity is accessible for anion transport and the water sampled gives the chemistry of the free pore water. For the MX80 experiment, we see that without any pressure or temperature applied during the hydration phase of the experiments (Arrow 1, Fig. 5), the concentrations of Br and Cl increase, mainly due to the water uptake due to water adsorption by clay minerals. Because there is no movement of the solute during the equilibrium phase and because this phase lasted 90 days, we can expect that diffusion processes could drive the isotopic fractionation observed for both Cl and Br. Diffusion in clay pore waters requires circumnavigating clay particle stacks which considerably increases the distance/length ratio of the pathway (tortuosity) (Melkior et al, 2009). In our experiment, the expelled water contains more of the lighter Cl isotope which is in agreement with the diffusion mechanism. However, because the heavier Br isotope is found in this same water, another mechanism has to be considered, namely possible gravitational fractionation of Br isotopes. Gravitational settlement of heavier Br isotopes. It took a total of 90 days for the completion of the hydration and equilibration (fluid circulation) phase to be completed. Water was sampled at the end of the 90 days. During the fluid circulation phase, water was circulated from the pump connected at the top to the pump connected at the bottom, so that when compaction start, the expelled sample could be collected in the empty pump connected at the top. Therefore, the sample called 'initial water' comes from the pump connected at the bottom of the clay. Gravitational isotopic fractionation is seen in columns of oil and gas reservoirs, in hydrothermal fluids, in sediments and even trapped air (Bons and Gomaz Rivas, 2012; Shirdokar et al., 2003; Zang and Kroos, 2001, Guinta et al., 2017). This might also be the case for Br.

When compaction started, pore pressure was maintained with the full pump connected to the bottom of the clay, and the expelled samples were collected in the empty pump connected to the top of the clay. This may explain the change in direction of the arrows on Fig 5 from 'initial' composition to 'pore pressure' composition. With the first pressurization (Arrow 2, Fig.5), the free pore water is expelled. The dominant mechanism of transport should be advection, so isotopic fractionation due to the pressurization should remain limited. This early compaction corresponds to the most significant decrease in porosity. As we reduced porosity, the composition of the free water, enriched in Cl and Br, can be attributed to the anion exclusion effect. The isotopic composition in Br and Cl is actually the composition enriched in heavier Cl and lighter Br, as a result of the inverse fractionation observed in the hydration step. The largest volumes of water are expelled during early compaction and the composition of the expelled water is supposed to be that of the free water.

As compaction continues pore size continues to decrease. The interparticle porosity will decrease first while the interlayer porosity will remain more or less constant (Muurinen et al., 2004). When the dry bulk density surpasses 1300 kg.m^{-3} between 45 and 65 MPa, the interlayer porosity will also start to decrease (Van Loon et al., 2007). This further amplifies the anion exclusion and trapping effect. The water expelled is different in composition from the trapped water. Cl and Br concentrations decrease (Arrow 3, Fig. 5) in the water expelled because they are trapped in the porosity by the anion exclusion effect. In addition to being forced to travel via longer transport routes through the clay layer, anions become trapped inside the diminishing pore spaces as a function of the ion size. Diffusion processes are more likely responsible for isotope fractionation implying that lighter isotopes move faster. This is valid for Cl. For Br, it is the heavier (larger) isotope that is preferentially expelled. The efficiency of fractionation is linked to the rate at which an isotope can diffuse away from a repulsive charge (Phillips and Bentley, 1987). ^{35}Cl with higher ionic mobility would be more effectively repulsed by the charge barrier than ^{37}Cl. The heavier ^{37}Cl isotope is also slower to diffuse out of the DDL into the free water when the anions are excluded during increasing compaction (Celejewski et al., 2018) as theoretically, ^{37}Cl isotope associates more strongly with divalent cations which will preferentially remain sorbed (Schauble et al., 2003).

At the highest compaction steps (Arrow 4, Fig. 5), the effect of higher temperature has to be mentioned because this can lead to faster diffusion and potential mineral transformation. Cl and Br in the expelled water continue to decrease due to diminishing pore size, which can be enhanced by possible mineral precipitation at high temperature. In terms of isotopes the expelled water tends to be slightly enriched in heavier Cl isotope and more significantly enriched in lighter Br isotope.

In correspondence to the findings of Kharaka and Berry (1973); Lavastre et al., (2005); Van Loon et al., (2007); and Nakata et al., (2016), the results from this study emphasize that the surface chemistry of the clay is a key factor in the efficiency of the clay to act as a filtration membrane. Smectite rich MX80, with a higher negative surface charge, was a more efficient filtration membrane for both Cl and Br anions compared to the illite-rich SSM, despite the SSM having been compacted to a much lower porosity than the MX80.

4.6 The case of Br

While Cl and Br are not significantly fractionated in the MX-80 experiment, Cl/Br ratio shows small but significant (i.e. beyond analytical uncertainties) fractionation from the early stage to the last step of the experiment compared to the original Bidart ocean water. In this experiment the freshening observed is therefore not only a result of retardation of dissolved solutes (filtration) but rather a result of trapping of the solutes by the clay layer itself. This trapping of the anions within the clay layer is a combination of both physical and chemical interaction between the clay mineral surfaces and the pore fluid.

Compaction of MX80 caused isotopic fractionation of Cl and of Br. Larger fractionation was observed for Br. The SSM compaction did not result in fractionation of Cl isotopes. However, compaction of the SSM caused Br isotope fractionation to the same extent as the MX80 compaction. This result suggests that Br was more readily fractionated compared to Cl. This result also supports the idea that fractionation is a result of both physical and chemical water-rock interactions, i.e. diminishing porosity and diffusion. However, the range of fractionation achieved during the clay compactions is smaller than what is measured in formation waters (up to - 8‰ for δ^{37}Cl and 4‰ for δ^{81}Br (Bagheri et al., 2014), due to the much smaller scale of the compaction experiment.

Considering the bromine isotope evolution Kharaka and Berry (1973) found that Br is filtered more effectively by a thin clay membrane compared to Cl due to its higher hydrated ionic potential (a function of charge and radius). The repulsive force created by charge barriers in negatively charged clay under compaction, will therefore generally be stronger on Br than on

Cl (and so retardation/preferential expulsion will be more prevalent). In addition, the relatively low concentration of Br compared to Cl (in natural formation waters), any slight uptake or release of Br may significantly affect the bromide concentration (and in effect also the isotopic composition) (Fontes and Matray, 1993; Bozau et al., 2015). What we see here is that it translates into amplified isotope fractionation of Br.

For the SSM compaction experiment, despite no change in concentration, Br isotopes were effectively fractionated. Br is the larger ion and has lower mobility compare to both Cl isotopes. The fractionation of Br during compaction might be more sensitive to decreasing porosity than Cl. This notion is supported by the isotopic fractionation for Br observed in the water remaining in the pore pressure generator pump after the SSM compaction (and not in the MX-80 compaction).

5. CONCLUSION

Our study on the chemical and isotopic fractionation of Cl and Br in water expelled during experimental compaction of clays, showed that they can help to reveal the history of pore fluids in sedimentary basins.

Despite showing no significant mineralogical transformations in terms of dissolution/precipitation processes, our experiment showed effective freshening and fractionation of Cl and Br isotopes. The range of freshening and fractionation observed in our experiments is in line with, but smaller than what is measured in natural samples. This is due to the extremely short time of the experiment (compared to geological time) and small volume of expelled water produced during the compaction. In particular, we suggest that:

1. Anion and isotope evolution during the compaction of clays is a function of both chemical and physical water-rock interactions. The surface chemistry of the clay in

combination with decreasing porosity result in re-equilibration of compressed and overlapping diffuse double layers which, in part, drive the anion and isotope evolution.

2. The clay with more negative surface charge is more effective in ultrafiltration/freshening of water expelled during compaction irrespective of its degree of compaction.
3. Reduction in porosity and the resulting charge barrier created due to overlapping of DDL's causes anions to become trapped in the clay layer. The retention effect is slightly more pronounced for Br than for Cl. This retention can explain the high salinities that are observed in flowback waters produced within the shales after hydraulic fracturing in gas shale exploitations.
4. Longer transport routes did not have a significant effect on the concentration of anions in the expelled water but did have a significant effect on the isotope composition due to diffusion processes.
5. The range of isotopic fractionation observed for Br is larger than what is seen for Cl.
6. The charge barrier resulting from compaction of negatively charged clays caused preferential expulsion of the heavier isotope for Cl and the lighter isotope for Br.
7. Fractionation of Cl isotopes is more prevalent during the earlier compaction steps (lower pressures and temperatures). Fractionation of Br isotopes becomes more pronounced at the later compaction steps (higher pressures and temperatures).

ACKNOWLEDGEMENTS

This work was funded by the Centre de Recherches sur la Géologie des Matières Premières Minérales et Energétiques (CREGU), Project Reference number: FR00008990 / T30, and

TOTAL EP-R&D. From the IPGP, Pierre Burckel is thanked for the ICP-MS analyses. From the GeoRessources laboratory; Laurent Schoumacker is thanked for the mercury intrusion porosimetry measurements.

The contribution of HGME is funded in part through the European Union's Horizon 2020 research and innovation programme under the Marie Skłodowska-Curie grant agreement No 702001 (BRISOACTIONS) and in part through the German Research Council (DFG) under grant no. MA2563-13.

REFERENCES

Agrinier, P., Destrigneville, C., Giunta, T., Bonifacie, M., Bardoux, G., Andre, J., & Lucazeau, F. (2019). Strong impact of ion filtration on the isotopic composition of chlorine in young clay-rich oceanic sediment pore fluids. *Geochimica et Cosmochimica Acta*, *245*, 525-541. https://doi.org/10.1016/j.gca.2018.11.013

Agrinier P., Bonfacie M., Bardoux G., Lucazeau F., Giunta T. and Ader M. (2021) Chlorine isotope data of chlorides challenge the pore fluid paradigm. *Geochimica et Cosmochimica Acta* , 300, 258-278. https://doi.org/10.1016/j.gca.2021.02.034

Appelo, C. A. J., Van Loon, L. R., & Wersin, P. (2010). Multicomponent diffusion of a suite of tracers (HTO, Cl, Br, I, Na, Sr, Cs) in a single sample of Opalinus Clay. Geochimica et Cosmochimica Acta, 74(4), 1201-1219.

Bagheri, R., Nadri, A., Raeisi, E., Eggenkamp, H. G. M., Kazemi, G. A., & Montaseri, A. (2014). Hydrochemical and isotopic (δ^{18}O, δ^{2}H, ^{87}Sr/^{86}Sr, δ^{37}Cl and δ^{81}Br) evidence for the origin of saline formation water in a gas reservoir. *Chemical Geology*, *384*, 62-75.

Bahnan, A. E., Carpentier, C., Pironon, J., Ford, M., Ducoux, M., Barré, G., ... & Gaucher, E. C. (2020). Impact of geodynamics on fluid circulation and diagenesis of carbonate reservoirs in a foreland basin: Example of the Upper Lacq reservoir (Aquitaine basin, SW France). *Marine and Petroleum Geology*, *111*, 676-694.

Balan, E., Créon, L., Sanloup, C., Aléon, J., Blanchard, M., Paulatto, L., & Bureau, H. (2019). First-principles modeling of chlorine isotope fractionation between chloride-bearing molecules and minerals. *Chemical Geology*, *525*, 424-434.

Beekman, H. E., Eggenkamp, H. G. M., & Appelo, C. A. J. (2011). An integrated modelling approach to reconstruct complex solute transport mechanisms–Cl and δ^{37}Cl in pore water of sediments from a former brackish lagoon in The Netherlands. *Applied geochemistry*, *26*(3), 257-268.

Bernachot, I., Garcia, B., Ader, M., Peysson, Y., Rosenberg, E., Bardoux, G., & Agrinier, P. (2017). Solute transport in porous media during drying: The chlorine isotopes point of view. *Chemical Geology*, *466*, 102-115.

Bethke, C. M., & Marshak, S. (1990). Brine migrations across North America—The plate tectonics of groundwater. *Annual Review of Earth and Planetary Sciences*, *18*(1), 287-315.

Bolt, G.H. and De Haan, F.A.M. (1982) Anion exclusion in soil. In: Bolt, G.H. (Ed.), Soil Chemistry: B. Physico-chemical Models. Elsevier, Amsterdam.

Bons, P. D., & Gomez-Rivas, E. (2013). Gravitational fractionation of isotopes and dissolved components as a first-order process in crustal fluids. *Economic Geology*, *108*(5), 1195-1201.

Bourg, I. C., Sposito, G., & Bourg, A. (2006). Tracer diffusion in compacted, water-saturated bentonite. *Clays and Clay Minerals*, *54*(3), 363-374.

Bozau, E., Sattler, C. D., & van Berk, W. (2015). Hydrogeochemical classification of deep formation waters. *Applied Geochemistry*, *52*, 23-30.

Bradbury, M. H., & Baeyens, B. (1998). A physicochemical characterisation and geochemical modelling approach for determining porewater chemistries in argillaceous rocks. *Geochimica et Cosmochimica Acta*, *62*(5), 783-795.

Bradbury, M. H., & Baeyens, B. (2003). Porewater chemistry in compacted re-saturated MX-80 bentonite. *Journal of Contaminant Hydrology*, *61*(1-4), 329-338.

Brady, N. C., Weil, R. R., & Weil, R. R. (2008). *The nature and properties of soils* (Vol. 13, pp. 662-710). Upper Saddle River, NJ: Prentice Hall.

Brigatti, M. F., Galan, E., & Theng, B. K. G. (2013). Structure and mineralogy of clay minerals. In *Developments in clay science* (Vol. 5, pp. 21-81). Elsevier.

Campbell, D. J. (1985). *FRACTIONATION OF STABLE CHLORINE ISOTOPES DURING TRANSPORT THROUGH SEMIPERMEABLE MEMBRANES* (Doctoral dissertation, The University of Arizona).

Carpenter, A. B. (1978, October). Origin and chemical evolution of brines in sedimentary basins. In *SPE Annual Fall Technical Conference and Exhibition*. OnePetro.

Celejewski, M., Barton, D., & Al, T. (2018). Measurement of Cl^-: Br^- Ratios in the Porewater of Clay-Rich Rocks—A Comparison of the Crush-and-Leach and the Paper-Absorption Methods. *Geofluids*, *2018*.

Coleman, M. L. (1992). Water composition variation within one formation. In *International symposium on water-rock interaction* (pp. 1109-1112).

Coplen, T. B., & Hanshaw, B. B. (1973). Ultrafiltration by a compacted clay membrane—I. Oxygen and hydrogen isotopic fractionation. *Geochimica et Cosmochimica Acta, 37*(10), 2295-2310.

Davis, S. N., Whittemore, D. O., & Fabryka-Martin, J. (1998). Uses of chloride/bromide ratios in studies of potable water. *Groundwater, 36*(2), 338-350.

Demir, I. (1988). Studies of smectite membrane behavior Electrokinetic, osmotic, and isotopic fractionation processes at elevated pressures. *Geochimica et Cosmochimica Acta*, *52*(3), 727-737.

Desaulniers, D. E., Kaufmann, R. S., Cherry, J. A., & Bentley, H. W. (1986). ^{37}Cl-^{35}Cl variations in a diffusion-controlled groundwater system. *Geochimica et Cosmochimica Acta*, *50*(8), 1757-1764.

Descostes, M., Blin, V., Bazer-Bachi, F., Meier, P., Grenut, B., Radwan, J., ... & Tevissen, E. (2008). Diffusion of anionic species in Callovo-Oxfordian argillites and Oxfordian limestones (Meuse/Haute–Marne, France). *Applied Geochemistry*, *23*(4), 655-677.

Eggenkamp, H. G. M. (1994). $\delta^{37}Cl$: The geochemistry of chlorine isotopes (Ph. D. thesis, Utrecht, Universiteit Utrecht).

Eggenkamp, H. G. M. (2014)a. A closer look at chlorine and bromine isotopes; An approach to understand the similarities and differences. *Journal of Biology and Earth Sciences*, *4*.

Eggenkamp, H. (2014)b. *The geochemistry of stable chlorine and bromine isotopes* (pp. 127-130). Berlin: Springer.

Eggenkamp, H. G. M., Bonifacie, M., Ader, M., & Agrinier, P. (2016). Experimental determination of stable chlorine and bromine isotope fractionation during precipitation of salt from a saturated solution. *Chemical Geology*, *433*, 46-56.

Eggenkamp, H. G. M., & Coleman, M. L. (2009). The effect of aqueous diffusion on the fractionation of chlorine and bromine stable isotopes. *Geochimica et Cosmochimica Acta*, *73*(12), 3539-3548.

Eggenkamp, H. G. M., Kreulen, R., & Van Groos, A. K. (1995). Chlorine stable isotope fractionation in evaporites. *Geochimica et Cosmochimica Acta*, *59*(24), 5169-5175.

Eggenkamp, H. G. M., Bonifacie, M., Ader, M., & Agrinier, P. (2016). Experimental determination of stable chlorine and bromine isotope fractionation during precipitation of salt from a saturated solution. *Chemical Geology*, *433*, 46-56.

Eggenkamp, H. G. M., & Louvat, P. (2018). A simple distillation method to extract bromine from natural water and salt samples for isotope analysis by multi-collector inductively coupled plasma mass spectrometry. *Rapid Communications in Mass Spectrometry*, *32*(8), 612-618.

Eggenkamp, H. G. M., Louvat, P., Agrinier, P., Bonifacie, M., Bekker, A., Krupenik, V., ... & Bagheri, R. (2019). The bromine and chlorine isotope composition of primary halite deposits and their significance for the secular isotope composition of seawater. *Geochimica et Cosmochimica Acta*, *264*, 13-29.

Fontes J.C. & Mantray J.M. (1993) Geochemistry and origin of formation brines from the Paris Basin, France; 1. Brines associated with Triassic salts. Chem. Geol. 109, 149-175.

Garven, G. (1995). Continental-scale groundwater flow and geologic processes. *Annual Review of Earth and Planetary Sciences*, *23*(1), 89-117.

Godon A., Jendrzejewski N., Eggenkamp H. G. M., Banks D. A., Ader M., Coleman M. L. and Pineau F. (2004) A crosscalibration of chlorine isotopic measurements and suitability of seawater as the international reference material. *Chemical Geology*, 207(1-2), 1–12.

Hanor, J. S., & Hanor, J. S. (1987). Origin and migration of subsurface sedimentary brines.

Haydon, P. R., & Graf, D. L. (1986). Studies of smectite membrane behavior: temperature dependence, 20–180° C. *Geochimica et Cosmochimica Acta*, *50*(1), 115-121.

Hendry, M. J., Wassenaar, L. I., & Kotzer, T. (2000). Chloride and chlorine isotopes (^{36}Cl and δ^{37}Cl) as tracers of solute migration in a thick, clay-rich aquitard system. *Water Resources Research*, *36*(1), 285-296.

Hesse, R., Egeberg, P. K., & Frape, S. K. (2006). Chlorine stable isotope ratios as tracer for pore-water advection rates in a submarine gas-hydrate field: implication for hydrate concentration. *Geofluids*, *6*(1), 1-7.

Karnland, O., Olsson, S., Nilsson, U., & Sellin, P. (2007). Experimentally determined swelling pressures and geochemical interactions of compacted Wyoming bentonite with highly alkaline solutions. *Physics and Chemistry of the Earth, Parts A/B/C*, *32*(1-7), 275-286.

Kaufmann, R., Long, A., Bentley, H., & Davis, S. (1984). Natural chlorine isotope variations. *Nature*, *309*(5966), 338-340.

Kendrick, M. A., Phillips, D., Wallace, M., & Miller, J. M. (2011). Halogens and noble gases in sedimentary formation waters and Zn–Pb deposits: A case study from the Lennard Shelf, Australia. *Applied Geochemistry*, *26*(12), 2089-2100.

Kharaka, Y. K., & Berry, F. A. (1973). Simultaneous flow of water and solutes through geological membranes—I. Experimental investigation. *Geochimica et Cosmochimica Acta*, *37*(12), 2577-2603.

Kharaka Y.K. & Hanor J.S. (2003). Deep fluids in the continents: I. Sedimentary basins. In: Drever, J.I., Holland, H.D., Turekian, K.K. (Eds.), Treatise in Geochemistry 5, 499–540.

Kozaki, T., Saito, N., Fujishima, A., Sato, S., & Ohashi, H. (1998). Activation energy for diffusion of chloride ions in compacted sodium montmorillonite. *Journal of Contaminant Hydrology*, *35*(1-3), 67-75.

Langmuir, I. (1918). The adsorption of gases on plane surfaces of glass, mica and platinum. *Journal of the American Chemical society*, *40*(9), 1361-1403.

Lavastre, V., Jendrzejewski, N., Agrinier, P., Javoy, M., & Evrard, M. (2005). Chlorine transfer out of a very low permeability clay sequence (Paris Basin, France): ^{35}Cl and ^{37}Cl evidence. *Geochimica et Cosmochimica Acta*, *69*(21), 4949-4961.

Lindemann, F. A. (1921). In discussion of isotopes. *Proc. Roy. Soc. Lond. Ser. A*, *99*, 102-104.

Louvat, P., Bonifacie, M., Giunta, T., Michel, A., & Coleman, M. (2016). Determination of bromine stable isotope ratios from saline solutions by “wet plasma” MC-ICPMS Including a comparison between high-and low-resolution modes, and three introduction systems. *Analytical chemistry*, *88*(7), 3891-3898.

Luo, C., Xiao, Y., Wen, H., Ma, H., Ma, Y., Zhang, Y., ... & He, M. (2014). Stable isotope fractionation of chlorine during the precipitation of single chloride minerals. *Applied geochemistry*, *47*, 141-149.

Melkior, T., Gaucher, E. C., Brouard, C., Yahiaoui, S., Thoby, D., Clinard, C., ... & Coelho, D. (2009). Na+ and HTO diffusion in compacted bentonite: Effect of surface chemistry and related texture. *Journal of Hydrology*, *370*(1-4), 9-20.

Molera, M., & Eriksen, T. (2002). Diffusion of $^{22}Na^{+}$, $^{85}Sr^{2+}$, $^{134}Cs^{+}$ and $^{57}Co^{2+}$ in bentonite clay compacted to different densities: experiments and modeling. *Radiochimica Acta*, *90*(9-11), 753-760.

Mondol, N. H., Bjørlykke, K., Jahren, J., & Høeg, K. (2007). Experimental mechanical compaction of clay mineral aggregates—Changes in physical properties of mudstones during burial. *Marine and petroleum geology*, *24*(5), 289-311.

Musashi, M., Oi, T., & Eggenkamp, H. G. (2004). Experimental determination of chlorine isotope separation factor by anion-exchange chromatography. *Analytica chimica acta*, *508*(1), 37-40.

Muurinen, A., Karnland, O., & Lehikoinen, J. (2004). Ion concentration caused by an external solution into the porewater of compacted bentonite. *Physics and Chemistry of the Earth, Parts A/B/C*, *29*(1), 119-127.

Nakata, K., Hasegawa, T., Higashihara, T., & Oyama, T. (2016). Chloride ion concentrations during the compression of rocks to extract pore water. *Geofluids*, *16*(1), 78-88.

Neaman, A., Pelletier, M., & Villieras, F. (2003). The effects of exchanged cation, compression, heating and hydration on textural properties of bulk bentonite and its corresponding purified montmorillonite. *Applied Clay Science*, *22*(4), 153-168.

Neuzil, C. E., & Person, M. (2017). Reexamining ultrafiltration and solute transport in groundwater. *Water Resources Research*, *53*(6), 4922-4941.

Nygård, R., Gutierrez, M., Gautam, R., & Høeg, K. (2004). Compaction behavior of argillaceous sediments as function of diagenesis. *Marine and Petroleum Geology*, *21*(3), 349-362.

Phillips, F. M., & Bentley, H. W. (1987). Isotopic fractionation during ion filtration: I. Theory. *Geochimica et Cosmochimica Acta*, *51*(3), 683-695.

Plecis, A., Schoch, R. B., & Renaud, P. (2005). Ionic transport phenomena in nanofluidics: experimental and theoretical study of the exclusion-enrichment effect on a chip. *Nano letters*, *5*(6), 1147-1155.

Pusch, R., Karnland, O., & Hökmark, H. (1990). *GMM-a general microstructural model for qualitative and quantitative studies of smectite clays* (No. SKB-TR--90-43). Swedish Nuclear Fuel and Waste Management Co.

Revil, A., & Leroy, P. (2004). Constitutive equations for ionic transport in porous shales. *Journal of Geophysical Research: Solid Earth*, *109*(B3).

Richard, A., Banks, D. A., Mercadier, J., Boiron, M. C., Cuney, M., & Cathelineau, M. (2011). An evaporated seawater origin for the ore-forming brines in unconformity-related uranium deposits (Athabasca Basin, Canada): Cl/Br and δ37Cl analysis of fluid inclusions. *Geochimica et Cosmochimica Acta*, *75*(10), 2792-2810.

Richard, A., Kendrick, M. A., & Cathelineau, M. (2014). Noble gases (Ar, Kr, Xe) and halogens (Cl, Br, I) in fluid inclusions from the Athabasca Basin (Canada): Implications for unconformity-related U deposits. Precambrian Research 247, 110-125.

Richet, P., Bottinga, Y., & Javoy, M. (1977). A review of hydrogen, carbon, nitrogen, oxygen, sulphur, and chlorine stable isotope fractionation among gaseous molecules. *Annual Review of Earth and Planetary Sciences*, *5*(1), 65-110.

Sato, H., Ashida, T., Kohara, Y., Yui, M., & Sasaki, N. (1992). Effect of dry density on diffusion of some radionuclides in compacted sodium bentonite. *Journal of Nuclear Science and Technology*, *29*(9), 873-882.

Sauzeat, E., Guillaume, D., Neaman, A., Dubessy, J., François, M., Pfeiffert, C., ... & Cathelineau, M. (2001). Caractérisation minéralogique, cristallochimique et texturale de l'argile MX80, Rapport ANDRA No. *RP. 0LEM*, 01-001.

Schauble, E. A. (2004). Applying stable isotope fractionation theory to new systems. *Reviews in mineralogy and geochemistry*, *55*(1), 65-111.

Schauble, E. A., Rossman, G. R., & Taylor Jr, H. P. (2003). Theoretical estimates of equilibrium chlorine-isotope fractionations. *Geochimica et Cosmochimica Acta*, *67*(17), 3267-3281.

Shackelford, C. D., & Daniel, D. E. (1991). Diffusion in saturated soil. II: Results for compacted clay. *Journal of Geotechnical Engineering*, *117*(3), 485-506.

Shirodkar, P. V., Xiao, Y. K., & Hai, L. (2003). Boron and chlorine isotopic signatures of seawater in the Central Indian Ridge. *Current Science*, 313-320.

Shouakar-Stash, O., Alexeev, S. V., Frape, S. K., Alexeeva, L. P., & Drimmie, R. J. (2007). Geochemistry and stable isotopic signatures, including chlorine and bromine isotopes, of the deep groundwaters of the Siberian Platform, Russia. *Applied geochemistry*, *22*(3), 589-605.

Solley, W. B., & Chase, E. B. (1983). Estimated use of water in the United States in 1980.

Stotler, R. L., Frape, S. K., & Shouakar-Stash, O. (2010). An isotopic survey of δ^{81}Br and δ^{37}Cl of dissolved halides in the Canadian and Fennoscandian Shields. *Chemical Geology*, *274*(1-2), 38-55.

Tournassat, C., & Appelo, C. A. J. (2011). Modelling approaches for anion-exclusion in compacted Na-bentonite. *Geochimica et Cosmochimica Acta*, *75*(13), 3698-3710.

Tremosa, J., Gailhanou, H., Chiaberge, C., Castilla, R., Gaucher, E. C., Lassin, A., ... & Claret, F. (2020). Effects of smectite dehydration and illitisation on overpressures in sedimentary basins: A coupled chemical and thermo-hydro-mechanical modelling approach. *Marine and Petroleum Geology*, *111*, 166-178.

Urey, H. C. (1947). The thermodynamic properties of isotopic substances. *Journal of the Chemical Society (Resumed)*, 562-581.

Van Loon, L. R., Glaus, M. A., & Müller, W. (2007). Anion exclusion effects in compacted bentonites: towards a better understanding of anion diffusion. *Applied Geochemistry*, *22*(11), 2536-2552.

Van Loon, L. R., Soler, J. M., Müller, W., & Bradbury, M. H. (2004). Anisotropic diffusion in layered argillaceous rocks: a case study with Opalinus Clay. *Environmental science & technology*, *38*(21), 5721-5728.

Wersin, P., Curti, E., & Appelo, C. A. J. (2004). Modelling bentonite–water interactions at high solid/liquid ratios: swelling and diffuse double layer effects. *Applied Clay Science*, *26*(1-4), 249-257.

Wigger, C., & Van Loon, L. R. (2017). Importance of interlayer equivalent pores for anion diffusion in clay-rich sedimentary rocks. *Environmental science & technology*, *51*(4), 1998-2006.

Worden, R. H. (1996). Controls on halogen concentrations in sedimentary formation waters. *Mineralogical Magazine*, *60*(399), 259-274.

Zhang, T., & Krooss, B. M. (2001). Experimental investigation on the carbon isotope fractionation of methane during gas migration by diffusion through sedimentary rocks at elevated temperature and pressure. *Geochimica et Cosmochimica Acta*, *65*(16), 2723-2742.

Clay compaction leads to expelled water freshening

Clay compaction leads to Cl and Br isotopes fractionation

Ultrafiltration is more effective for clay with the more negative surface charge

The retention effect in clay porosity is slightly more pronounced for Br than for Cl

Declaration of interests

☒ The authors declare that they have no known competing financial interests or personal relationships that could have appeared to influence the work reported in this paper.

☐The authors declare the following financial interests/personal relationships which may be considered as potential competing interests: